PHYSICAL REVIEW D **95,** 014003 (2017)

$\gamma^* N \to N^*(1520)$ form factors in the timelike regime

G. Ramalho[1] and M. T. Peña[2]

[1]*International Institute of Physics, Federal University of Rio Grande do Norte, Campus Universitário—Lagoa Nova, C.P. 1613, Natal, Rio Grande do Norte 59078-970, Brazil*

[2]*Centro de Física Teórica e de Partículas (CFTP), Instituto Superior Técnico (IST), Universidade de Lisboa, Avenida Rovisco Pais, 1049-001 Lisboa, Portugal*

(Received 28 October 2016; published 5 January 2017)

The covariant spectator quark model, tested before in a variety of electromagnetic baryon excitations, is applied here to the $\gamma^* N \to N^*(1520)$ reaction in the timelike regime. The transition form factors are first parametrized in the spacelike region in terms of a valence quark core model together with a parametrization of the meson cloud contribution. The form factor behavior in the timelike region is then predicted, as well as the $N^*(1520) \to \gamma N$ decay width and the $N^*(1520)$ Dalitz decay, $N^*(1520) \to e^+e^-N$. Our results may help in the interpretation of dielectron production from elementary pp collisions and from the new generation of HADES results using a pion beam. In the $q^2 = 0$–1 GeV^2 range, we conclude that the *QED approximation* (a q^2 independent form factor model) underestimates the electromagnetic coupling of the $N^*(1520)$ from 1 up to 2 orders of magnitude. We conclude also that the $N^*(1520)$ and $\Delta(1232)$ Dalitz decay widths are comparable.

DOI: 10.1103/PhysRevD.95.014003

I. INTRODUCTION

Measurements of dielectron production in elementary pp collisions [1–7] expand to the timelike region ($q^2 > 0$, where q is the momentum transfer) the extraordinarily precise results obtained with the electron scattering CLAS N^* program at Jefferson Lab [1,8,9], describing the electromagnetic structure of baryonic transitions in a spacelike or $q^2 < 0$ region (a program to be extended down to -12 GeV^2, as well as up to -0.05 GeV^2). Although different, both experiments, with strong and electromagnetic probes, complement each other [1].

In the last years, pp and quasifree pn reactions were combined for the determination of different medium effects, difficult to disentangle [10–12]. The dominance of the $\Delta(1232)$ Dalitz decay for dielectron emission above the π^0 mass was confirmed by HADES, by the simultaneous measurement of one pion-production channels [3,4]. However, an excess of production with respect to the baryon and meson cocktail simulations was observed, an effect pointing to the contribution of low-lying resonances, as the $N^*(1520)$ [3,13,14]. The important role of this state in dilepton decay reactions, as the $\gamma^* N \to e^+e^-N$, in the timelike region was also discussed in Refs. [2,15–17].

To focus on this contribution, very recently, the High Acceptance Di-Electron Spectrometer (HADES) at GSI was combined with a pion beam for perfect and unique cold matter studies [3–5]. The first pion beam results from HADES experiments [13,14] also show in the dielectron emission channel a large peak in the number of events in a missing mass range of 0.9–1.04 GeV^2, which is expected to be due to $N^*(1520)$ decay. The new experiments with HADES and a pion beam are an extraordinary opportunity to shed light on the behavior of the second and third resonance region, and the resonance form factors in the timelike region [3,13,14]. This motivates calculations, as the one reported here, for the extraction of different contributions to e^+e^- emission, as well as to revisit, in the electromagnetic couplings of baryons, the extensively applied vector meson dominance principle and its validity. To understand the structure of hadrons from first principles the nonperturbative character of QCD at low energies and chiral symmetry have to be combined [8]. In the two extreme regimes of QCD—the low-energy regime where the energies are (much) smaller than a typical strong interaction scale and the high-energy regime where the energies are much higher than that scale—well-established theoretical methods, chiral perturbation theory and perturbative QCD, respectively, apply [8]. However, in the intermediate-energy regime, some degree of modeling is still required.

Promising tools are Dyson-Schwinger-Faddeev functional methods and lattice QCD. Although progress in these fronts continues, they are developed in Euclidean space and, so far, are limited to the region below the ρ-meson pole [18]. At this stage, we take here a more phenomenological approach, based on the covariant spectator quark model. This model is based on the covariant spectator theory [19]. In a relatively successful and unifying way, our approach pictures a large variety of baryons as a superposition of a core of three valence quarks and meson cloud components [6–8,20–33]. After a series of applications of the model to the electromagnetic excitation of baryons in the spacelike regime, we analyzed also the impact of the $\Delta(1232)$ resonance in the timelike reactions [6,7].

 © 2017 American Physical Society

In this work we start with the quark model described in Ref. [20] for the $N^*(1520)$ resonance and extend it to the region $q^2 > 0$. In addition to the contribution from the bare core, we take also a meson cloud contribution. This contribution is modeled within the lines of our previous study of the $\Delta(1232)$ in the timelike region, i.e., with the pion-photon coupling parametrized by the pion form factor data [7].

Three conclusions emerged in the context of our model: (i) the $\gamma^* N \to N^*(1520)$ timelike transition form factors are dominated by the meson cloud contributions; (ii) in the range $q^2 = 0$–1 GeV^2, the constant form factor model (also known as *QED approximation*) usually taken in the literature underestimates the electromagnetic coupling of the $N^*(1520)$ with consequences for the differential Dalitz decay width; (iii) in addition to the $\Delta(1232)$ resonance, the $N^*(1520)$ has a role in dilepton decay reactions at intermediate energies.

This article is organized as follows. In Sec. II we describe the methodology used to extend a valence quark model fixed in the spacelike region to the timelike region. Next, in Sec. III, we discuss the relation between the $\gamma^* N \to N^*(1520)$ form factors and the formulas for the photon and Dalitz decay widths of the $N^*(1520)$. The formalism of the covariant spectator quark model used here is presented briefly in Sec. IV. In Sec. V we discuss the formulas used to calculate the $\gamma^* N \to N^*(1520)$ form factors. The results for the form factors in the timelike region and the $N^*(1520)$ decay widths are presented in Sec. VI. Outlook and conclusions are presented in Sec. VII.

II. METHODOLOGY

In the covariant spectator quark model, the application of impulse approximation to the interaction of a photon with a baryon, seen as a three quark qqq state, justifies that one integrates out the relative internal momentum in the spectator diquark subsystem [21,25,26]. After this internal momentum integration, in the process of the covariant integration over the global momentum of the interacting diquark, one may keep only the main contribution, which is originated by the on-mass-shell pole of the diquark—while the remaining quark that interacts with the photon is taken to be off mass shell [25]. This last integration on the on-shell diquark internal momenta amounts to having the qqq system as a quark-diquark system, and to treating the diquark with an effective average mass m_D [21,25,26]. It is also an ingredient of the model that the electromagnetic quark current is represented by a parametrization of vector meson dominance [21,26,34,35]. In addition to the contributions from the core of valence quarks, the covariant spectator quark model can include also a covariant parametrization of the meson cloud effects that are important in the low momentum transfer region and that depend on the baryons participating in the reaction [6,7,22,23,31,36–38].

Here, the extension of the model to the timelike regime requires two important modifications:

(i) The nucleon and the $N^*(1520)$ quark core wave functions have to be calculated in timelike kinematic conditions, depending on an arbitrary mass W which can differ from the resonance mass, labeled M_R.

(ii) The electromagnetic quark current has also to be extended to the timelike regime. That is done by introducing finite mass widths for the ρ and ω mesons.

For the $\gamma^* N \to \Delta(1232)$ transition in the timelike region, we have already found that the meson cloud contributions are important, in comparison to the valence quark contributions [7]. It is worthwhile now to test whether the same phenomena occurs for the $N^*(1520)$ resonance, which carries, in particular, a different isospin. In our model the valence quark contributions for the magnetic and electric form factors vanish at the photon point ($q^2 = 0$) due to the orthogonality of the initial and final state wave functions [20]. Other valence quark models estimate them as nonzero contributions (a discussion can be found in Ref. [20]). Since, in our model, the valence quark contributions for the electric and magnetic transition form factors vanish at $q^2 = 0$, their extension to the $q^2 > 0$ region gives nonzero but small contributions for those transition form factors. Nevertheless, our model can provide a good approximation for the $N^*(1520)$ resonance in the timelike region based on the meson cloud contributions, which dominate in the timelike region. Moreover, the form factors show a dependence on q^2 with consequences for the analysis of reactions in the timelike region, where the electromagnetic couplings are often fixed at their value at $q^2 = 0$ (the QED approximation).

III. $N^*(1520)$ DALITZ DECAY

The $N^*(1520)$ resonance is a $J^P = \frac{3}{2}^-$ state, with isospin $I = \frac{1}{2}$. The $N^*(1520)$ Dalitz decay into the nucleon can be expressed in terms of the decay width [39]

$$\Gamma_{\gamma^* N}(q, W) = \frac{3\alpha}{16}\frac{(W-M)^2}{M^2 W^3}\sqrt{y_+ y_-}\, y_+ |G_T(q^2, W)|^2, \quad (3.1)$$

where $q = \sqrt{q^2}$, α is the fine-structure constant,

$$y_\pm = (W \pm M)^2 - q^2, \quad (3.2)$$

and $|G_T(q^2, W)|^2$ is a combination of the electromagnetic transition form factors given by

$$|G_T(q^2, W)|^2 = 3|G_M(q^2, W)|^2 + |G_E(q^2, W)|^2 + \frac{q^2}{2W^2}|G_C(q^2, W)|^2. \quad (3.3)$$

In the previous equation G_M, G_E, and G_C are, respectively, the magnetic dipole, electric, and Coulomb quadrupole

form factors, which are complex functions in the region $q^2 > 0$.

The dilepton decay rate is obtained from the relation (3.1). Using the compact notation $\Gamma \equiv \Gamma_{e^+e^-N}$, one can calculate the dilepton decay rate [39,40] as

$$\Gamma'_{e^+e^-N}(q,W) \equiv \frac{d\Gamma}{dq}(q,W) = \frac{2\alpha}{3\pi q^3}(2\mu^2+q^2)\sqrt{1-\frac{4\mu^2}{q^2}}\Gamma_{\gamma^* N}(q,W), \tag{3.4}$$

where μ is the electron mass.

The Dalitz decay width is then determined by the integral of $\Gamma'_{e^+e^-N}(q,W)$ in the kinematic region $4\mu^2 \le q^2 \le (W-M)^2$:

$$\Gamma_{e^+e^-N}(W) = \int_{2\mu}^{W-M} \Gamma'_{e^+e^-N}(q,W)dq. \tag{3.5}$$

IV. COVARIANT SPECTATOR QUARK MODEL

In the covariant spectator quark model, the baryon wave functions are specified by the flavor, spin, orbital angular momentum, and radial excitations of the quark-diquark states that are consistent with the baryon quantum number [8,21,26,36]. The nucleon wave function Ψ_N was obtained in Ref. [21] and the wave function Ψ_R of the resonance $N^*(1520)$ in Ref. [20]. Those wave functions describe only the valence quark content of those baryons.

The constituent quark electromagnetic current is written as the sum of a Dirac and a Pauli component,

$$j^\mu_q(q) = \left(\frac{1}{6}f_{1+} + \frac{1}{2}f_{1-}\tau_3\right)\gamma^\mu + \left(\frac{1}{6}f_{2+} + \frac{1}{2}f_{2-}\tau_3\right)\frac{i\sigma^{\mu\nu}q_\nu}{2M}, \tag{4.1}$$

where τ_3 is the Pauli matrix that acts on the (initial and final) baryon isospin states, M is the nucleon mass, and $f_{i\pm}(q^2)$ are the quark isoscalar/isovector form factors. Those form factors will be parametrized with a form consistent with the vector meson dominance (VMD) mechanism.

For inelastic reactions, we replace $\gamma^\mu \to \gamma^\mu - \frac{\not{q} q^\mu}{q^2}$ in order to ensure the conservation of the transition current. This is equivalent to the Landau prescription [41–43]. The extra term restores current conservation but does not affect the results of the observables [41].

Once we know the wave functions for the nucleon $\Psi_N(P_-,k)$ and the resonance $\Psi_R(P_+,k)$, with momenta P_- and P_+, respectively, and the diquark momentum k, we can calculate the transition current in a relativistic impulse approximation [21,25,26]

$$J^\mu = 3\sum_\Gamma \int_k \bar{\Psi}_R(P_+,k) j^\mu_q \Psi_N(P_-,k), \tag{4.2}$$

where Γ represents the intermediate diquark polarizations, and the integration symbol represents the covariant integration over the diquark on-shell momentum. The factor 3 takes into account the contributions of all of the quark pairs. The polarization indices are suppressed in the wave functions just for simplicity. The current associated with the meson cloud will be parametrized separately and more phenomenologically, as discussed later. The two components of the current are conserved individually.

The definition (4.2) for the electromagnetic current is valid for the spacelike and timelike regions. In the rest frame of the resonance (mass W), we may write

$$P_- = (E_N, -\mathbf{q}), \qquad P_+ = (W, \mathbf{0}), \tag{4.3}$$

where $\mathbf{q}$ is the photon three-momentum. In that case, the magnitude of the three-vector $\mathbf{q}$ corresponding to a photon of the four-momentum q and the squared momentum q^2 is given by

$$|\mathbf{q}|^2 = \frac{y_+ y_-}{4W^2}, \tag{4.4}$$

where $y_\pm$ is defined in Eq. (3.2). In the case of a timelike photon ($q^2 > 0$), the last condition implies that physical photons (with $|\mathbf{q}|^2 \ge 0$) are defined only for $0 \le q^2 \le (W-M)^2$, or $q^2 \ge (W+M)^2$. As we are interested in resonance decay, the region near $q^2 = 0$ is the one upon which we will focus, and we will skip the discussion of the last case. In conclusion, because both the nucleon and the resonance are taken on their mass shell, the transition form factors for a transition between a nucleon of mass M and a resonance of mass W are kinematically restricted to the region $q^2 \le (W-M)^2$ in the timelike region. As the resonance mass W grows larger, the spanned momentum region increases.

A. Quark form factors

The valence quark form factors, included in the effective electromagnetic quark current (4.1) have a parametrization inspired in the VMD mechanism that reads [21,34,35]

$$f_{1\pm}(q^2) = \lambda_q + (1-\lambda_q)\frac{m^2_{v\pm}}{m^2_{v\pm}-q^2} - c_\pm \frac{M_h^2 q^2}{(M_h^2-q^2)^2},$$
$$f_{2\pm}(q^2) = \kappa_\pm\left\{d_\pm \frac{m^2_{v\pm}}{m^2_{v\pm}-q^2} + (1-d_\pm)\frac{M_h^2}{M_h^2-q^2}\right\}. \tag{4.5}$$

Here, $m_{v\pm}$ represents light vector meson masses, M_h is an effective heavy vector meson, $\kappa_\pm$ indicates the quark anomalous magnetic moment, $c_\pm, d_\pm$ are mixture coefficients, and λ_q is a high-energy parameter related to the quark density number in the deep inelastic limit [21]. For

the isoscalar functions, one has $m_{v+} = m_\omega$ (the ω mass) and, for the isovector functions, one uses $m_{v-} = m_\rho$ (the ρ mass). The term in $M_h = 2M$ simulates the effects of the heavier mesons and, therefore, all short-range physics.

Specifically, we used the quark current parametrization of model II from Ref. [21]: $\lambda_q = 1.21$, $c_+ = 4.16$, $c_- = 1.16$, $d_+ = d_- = -0.686$, $\kappa_+ = 1.639$, and $\kappa_- = 1.833$. The values were adjusted in order to describe the nucleon elastic form factor data in the spacelike region. (The radial wave functions are described later.) Its behavior in that region was tested by taking it to the lattice QCD regime [34,35], and also to the nuclear medium [38], both implemented with success.

However, some discussion is necessary for the timelike situation $q^2 > 0$. As seen from Eq. (4.5), singularities will appear when $q^2 = m_{v\pm}^2$. Physically, they correspond to the ρ and ω poles. Another singularity appears from the pole at $q^2 = M_h^2$, but only for very large q^2's ($\simeq 3.5$ GeV^2). The M_h pole was introduced for phenomenological reasons to parametrize the short-range physics in the spacelike region [21]. For calculations with large W's (large q^2's) the M_h pole has to be regularized as discussed in the Appendix.

The spacelike parametrization of the quark current in terms of the ω and ρ poles assumes that those particles are stable particles with zero decay width $\Gamma_v = 0$. In the extension of the quark form factors to the timelike regime we give them a width and use instead the substitution

$$\frac{m_v^2}{m_v^2 - q^2} \to \frac{m_v^2}{m_v^2 - q^2 - i m_v \Gamma_v(q^2)}, \tag{4.6}$$

where the index v is used for either ρ or ω as before. On the rhs, Γ_v denotes the vector meson decay width function in terms of q^2.

In the application to the $\Delta(1232)$ Dalitz decay [7], only the ρ pole was taken because, in the $\gamma^* N \to \Delta$ transition, only the isovector components contribute (given by the functions f_{i-}).

The function $\Gamma_\rho(q^2)$ represents the $\rho \to 2\pi$ decay width for a virtual ρ with a momentum q^2 [44,45],

$$\Gamma_\rho(q^2) = \Gamma_\rho^0 \frac{m_\rho^2}{q^2} \left(\frac{q^2 - 4m_\pi^2}{m_\rho^2 - 4m_\pi^2} \right)^{\frac{3}{2}} \theta(q^2 - 4m_\pi^2), \tag{4.7}$$

where $\Gamma_\rho^0 = 0.149$ GeV.

For the application in this paper, however, we also have to include the ω pole. To this end, the function $\Gamma_\omega(q^2)$ will include the decays $\omega \to 2\pi$ (function $\Gamma_{2\pi}$) and $\omega \to 3\pi$ (function $\Gamma_{3\pi}$). The case $\omega \to 3\pi$ can be interpreted as the process $\omega \to \rho\pi \to 3\pi$, and therefore we decomposed $\Gamma_\omega(q^2)$ into [44]

$$\Gamma_\omega(q^2) = \Gamma_{2\pi}(q^2) + \Gamma_{3\pi}(q^2). \tag{4.8}$$

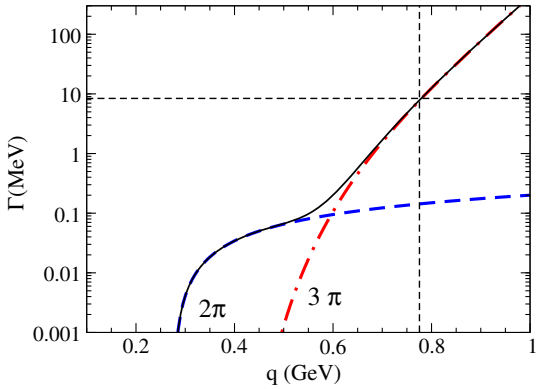

FIG. 1. Γ_ω as a function of q. The 2π, 3π channels are indicated by the long-dashed and dotted-dashed lines, respectively. The solid line represents the sum of the two channels. The short-dashed vertical and horizontal lines indicate the ω mass point and the ω-physical width (8.4 MeV).

The function $\Gamma_{2\pi}$ can be represented as [44,46]

$$\Gamma_{2\pi}(q^2) = \Gamma_{2\pi}^0 \frac{m_\omega^2}{q^2} \left(\frac{q^2 - 4m_\pi^2}{m_\omega^2 - 4m_\pi^2} \right)^{\frac{3}{2}} \theta(q^2 - 4m_\pi^2), \tag{4.9}$$

where $\Gamma_{2\pi}^0 = 1.428 \times 10^{-4}$ GeV. Note that $\Gamma_{2\pi}$ is similar to the function Γ_ρ except for the constant $\Gamma_{2\pi}^0$ (about 10^3 smaller) and the mass. For the function $\Gamma_{3\pi}$, we use the result from Ref. [44],

$$\Gamma_{3\pi}(q^2) = \int_{9m_\pi^2}^{(q-m_\pi)^2} ds \mathcal{A}_\rho(s) \bar{\Gamma}_{\omega\to\rho\pi}(q^2, s), \tag{4.10}$$

where $q = \sqrt{q^2}$, s the mass of the virtual ρ meson, $\bar{\Gamma}_{\omega\to\rho\pi}$ is the decay width of ω to a π and a virtual ρ, and $\mathcal{A}_\rho$ is the ρ-spectral function. The functions $\bar{\Gamma}_{\omega\to\rho\pi}$ and $\mathcal{A}_\rho$ are [44]

$$\bar{\Gamma}_{\omega\to\rho\pi}(q^2, s) = \frac{3}{4\pi} \left(\frac{g'}{m_\pi} \right)^2 \left[\frac{(q^2 - s - m_\pi^2)^2 - 4sm_\pi^2}{4q^2} \right]^{\frac{5}{2}} \times \theta(q^2 - 9m_\pi^2), \tag{4.11}$$

with $g' = 10.63$ MeV and

$$\mathcal{A}_\rho(s) = \frac{\sqrt{s}}{\pi} \frac{\Gamma_\rho(s)}{(s - m_\rho^2)^2 + s\Gamma_\rho^2(s)}. \tag{4.12}$$

With this parametrization, we obtain $\Gamma_\omega(m_\omega^2) \simeq \Gamma_{3\pi}(m_\omega^2) = 7.6$ MeV, which is consistent with the data. Note that the total width of the ω comprises the decays into $\gamma\pi$, 2π, and 3π and is 8.4 MeV. The remaining contribution to the ω decay width comes from the decay $\omega \to \gamma\pi^0$. The 3π decay corresponds to a branching ratio of about 90%.

The result of the calculation of Γ_ω as a function of q is shown in Fig. 1. Note in this figure the dominance of the 3π channel for $q > 0.55$ GeV.

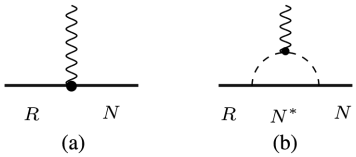

FIG. 2. Electromagnetic interaction (a) with the quark core and (b) with the meson cloud. The intermediate N^* is a octet baryon member (spin 1/2) or a decuplet baryon member (spin 3/2).

V. FORM FACTORS

Although the $\gamma^* N \to N^*(1520)$ transition is characterized by the three independent form factor functions G_M, G_E, and G_C, in the study of the reaction in the spacelike regime [20], we concluded that it is convenient to define an auxiliary form factor,

$$\tilde{G}_4 = G_E + G_M, \tag{5.1}$$

because the valence quark contributions for $\tilde{G}_4$ are zero and a direct extraction of the *pure* meson cloud contribution from the data therefore arises naturally (in the context of the covariant spectator quark model). The valence quark contributions for the transition form factors are discussed next.

Separating the valence quark contribution, represented in Fig. 2(a), from the meson cloud contribution, represented in Fig. 2(b), one can decompose each of the three form factors as in Ref. [20],

$$G_M(q^2, W) = G_M^B(q^2, W) + G_M^\pi(q^2), \tag{5.2}$$

$$G_E(q^2, W) = -G_M^B(q^2, W) - G_M^\pi(q^2) + \tilde{G}_4^\pi(q^2), \tag{5.3}$$

$$G_C(q^2, W) = G_C^B(q^2, W) + G_C^\pi(q^2), \tag{5.4}$$

where $G_X^B(q^2, W)$, $X = M, E, C$ give the valence quark core contributions and $G_M^\pi, \tilde{G}_4^\pi$, and G_C^π stand for the matching meson cloud contributions. The label π is used instead of MC (meson cloud) because we describe those contributions in terms of the pion electromagnetic form factor (following what was done for the $\gamma^* N \to \Delta$ transition [7,20]). The formulas for the valence quark core and meson cloud contributions will be given in the next sections.

Once the transition form factors are known, the helicity amplitudes can be calculated using

$$A_{1/2} = \frac{1}{F} G_M + \frac{1}{4F} \tilde{G}_4, \tag{5.5}$$

$$A_{3/2} = \frac{\sqrt{3}}{4F} \tilde{G}_4, \tag{5.6}$$

$$S_{1/2} = \frac{1}{\sqrt{2}F} \frac{|\mathbf{q}|}{2W} G_C, \tag{5.7}$$

where $F = \frac{1}{e} \frac{W}{|\mathbf{q}|} \sqrt{\frac{MK}{W} \frac{y_-}{(W-M)^2}}$, with $K = \frac{W^2 - M^2}{2W}$.

A. Valence quark form factors

The contributions of the valence quark core to the form factors can be calculated and seen to have the general final form [9,47]

$$G_M^B = -\mathcal{R}[(W-M)^2 - q^2] \frac{G_1}{W}, \tag{5.8}$$

$$G_E^B = -\mathcal{R}\left\{4G_4 - [(W-M)^2 - q^2] \frac{G_1}{W}\right\}, \tag{5.9}$$

$$G_C^B = -\mathcal{R}[4WG_1 + (3W^2 + M^2 - q^2)G_2 + 2(W^2 - M^2 + q^2)G_3], \tag{5.10}$$

where G_i $(i = 1, 2, 3)$ represents three independent form factors and $\mathcal{R} = \frac{1}{\sqrt{6}} \frac{M}{W-M}$. The function G_4 was introduced for convenience. Because of current conservation, G_4 is given in terms of three independent G_i's $(i = 1, 2, 3)$ as [20]

$$G_4 = (W-M)G_1 + \frac{1}{2}(W^2 - M^2)G_2 + q^2 G_3. \tag{5.11}$$

By combining the results for G_E and G_M, one concludes that the valence quark core contribution for $\tilde{G}_4$ is $\tilde{G}_4^B = G_E^B + G_M^B = -4\mathcal{R}G_4$.

The explicit calculation of the form factors requires the determination of the coefficients of the antisymmetric (A) and symmetric (S) components of the wave functions, in terms of the quark form factors

$$j_i^A = \frac{1}{6} f_{i+} + \frac{1}{2} f_{i-} \tau_3, \tag{5.12}$$

$$j_i^S = \frac{1}{6} f_{i+} - \frac{1}{6} f_{i-} \tau_3. \tag{5.13}$$

See Refs. [20,36] for more details.

Then, the functions G_i can be computed from the nucleon and resonance wave functions. The results are [20]

$$G_1 = -\frac{3}{2\sqrt{2}|\mathbf{q}|} \left[\left(j_1^A + \frac{1}{3} j_1^S\right) + \frac{W+M}{2M}\left(j_2^A + \frac{1}{3} j_2^S\right)\right] \mathcal{I}, \tag{5.14}$$

$$G_2 = \frac{3}{2\sqrt{2}M|\mathbf{q}|}\left[j_2^A + \frac{1}{3}\frac{1-3\tau}{1+\tau}j_2^S + \frac{4}{3}\frac{2M}{W+M}\frac{1}{1+\tau}j_1^S\right]\mathcal{I}, \tag{5.15}$$

$$G_3 = \frac{3}{2\sqrt{2}|\mathbf{q}|}\frac{W-M}{q^2}\left[j_1^A + \frac{1}{3}\frac{\tau-3}{1+\tau}j_1^S + \frac{4}{3}\frac{W+M}{2M}\frac{\tau}{1+\tau}j_2^S\right]\mathcal{I}, \tag{5.16}$$

where $\tau = -\frac{q^2}{(W+M)^2}$, and

$$\mathcal{I} = -\int_k \frac{(\varepsilon_{0P_+}\cdot\tilde{k})}{\sqrt{-\tilde{k}^2}}\psi_R(P_+,k)\psi_N(P_-,k). \tag{5.17}$$

The functions ψ_N and ψ_R in the formulas above are the nucleon and resonance radial wave functions, respectively; ε_{0P_+} is the spin-1 polarization vector and $\tilde{k} = k - \frac{P_+\cdot k}{W^2}P_+$ [20]. The previous integral is calculated in the resonance rest frame using the conditions given by Eq. (4.3).

From Eq. (5.11) one concludes, as mentioned before, that $G_4 \equiv 0$, implying that $G_E^B = -G_M^B$ and motivating the use of $\tilde{G}_4$ to extract direct information on the meson cloud since it, alone, contributes to $\tilde{G}_4$.

The consequence of the gauge invariant correction to Eq. (4.1) is that in the Dirac part of the current, G_3, is determined from G_1 and G_2, and G_3 becomes nonzero at $q^2 = 0$ [20]. Importantly, the Dirac contribution for G_3 is responsible for the nonvanishing value of G_C at $q^2 = 0$. This is similar to the $\Delta(1232)$ case addressed in Ref. [23].

The radial wave functions ψ_N and ψ_R are parametrized phenomenologically as in Ref. [20] for the $N^*(1520)$ resonance, and as in Ref. [21] for the nucleon. Those functions depend on $P\cdot k$, where P is the momentum of the baryon. More specifically, those functions can be expressed as functions of the dimensionless variable χ which, in the nonrelativistic limit, becomes proportional to $\mathbf{k}^2$ [26] and is defined as

$$\chi_B = \frac{(M_B - m_D)^2 - (P-k)^2}{M_B m_D}, \tag{5.18}$$

where M_B is the mass of the baryon.

The nucleon radial wave function is represented as [21]

$$\psi_N(P,k) = \frac{N_0}{m_D(\beta_1+\chi_N)(\beta_2+\chi_N)}, \tag{5.19}$$

where β_1 and β_2 are two momentum range parameters and N_0 is the normalization constant. We choose $\beta_2 > \beta_1$; therefore, β_2 regulates the long-range behavior in the configuration space. In the numerical calculations, we used $\beta_1 = 0.049$ and $\beta_2 = 0.717$ [21].

For the $N^*(1520)$ state, we used [20]

$$\psi_R(P,k) = \frac{N_1}{m_D(\beta_2+\chi_R)}\left[\frac{1}{(\beta_1+\chi_R)} - \frac{\lambda_R}{(\beta_3+\chi_R)}\right], \tag{5.20}$$

where N_1 is the normalization constant, β_3 is a new (short-range) parameter, and λ_R is a parameter determined by an orthogonality condition between the nucleon and the $N^*(1520)$ wave functions. As in Ref. [20], we use here $\beta_3 = 0.257$. The orthogonality condition for wave functions of the nucleon and its excitation is given by $\mathcal{I}(0) = 0$, where $\mathcal{I}(Q^2)$ is defined by Eq. (5.17) [20].

The parameters of the nucleon radial wave function were determined by the direct fit to the nucleon form factor data, in a model with no meson cloud [21]. The parameters of the $N^*(1520)$ radial wave function were determined by the fit to the $\gamma^*N \to N^*(1520)$ data for $Q^2 = -q^2 > 1.5$ GeV^2, a region where the meson cloud effects are expected to be very small [20].

The radial wave functions ψ_N and ψ_R are normalized, by imposing the conditions ($B = N$, R)

$$\int_k |\psi_B(\bar{P},k)|^2 = 1, \tag{5.21}$$

where $\bar{P} = (M_B, 0, 0, 0)$ is the baryon momentum in the rest frame (M_N represents the nucleon mass). Equation (5.21) ensures the right charge for each of the baryons B, obtained from the operator $\frac{1}{2}(1+\tau_3)$ [20,21].

B. Meson cloud form factors

The meson cloud form factors can be represented as in Ref. [20],

$$\tilde{G}_4^\pi(q^2) = \lambda_\pi^{(4)}\left(\frac{\Lambda_4^2}{\Lambda_4^2 - q^2}\right)^3 F_\pi(q^2)\tau_3, \tag{5.22}$$

$$G_M^\pi(q^2) = (1 - a_M q^2)\lambda_\pi^M\left(\frac{\Lambda_M^2}{\Lambda_M^2 - q^2}\right)^3 F_\pi(q^2)\tau_3, \tag{5.23}$$

$$G_C^\pi(q^2) = \lambda_\pi^C\left(\frac{\Lambda_C^2}{\Lambda_C^2 - q^2}\right)^3 F_\pi(q^2)\tau_3, \tag{5.24}$$

where $F_\pi(q^2)$ is a parametrization of the pion electromagnetic form factors determined in Ref. [7]. Specifically, we use the form

$$F_\pi(q^2) = \frac{\alpha}{\alpha - q^2 - \frac{1}{\pi}\beta q^2 \log\frac{q^2}{m_\pi^2} + i\beta q^2}, \tag{5.25}$$

where $\alpha = 0.696$ GeV^2, $\beta = 0.178$, and m_π is the pion mass.

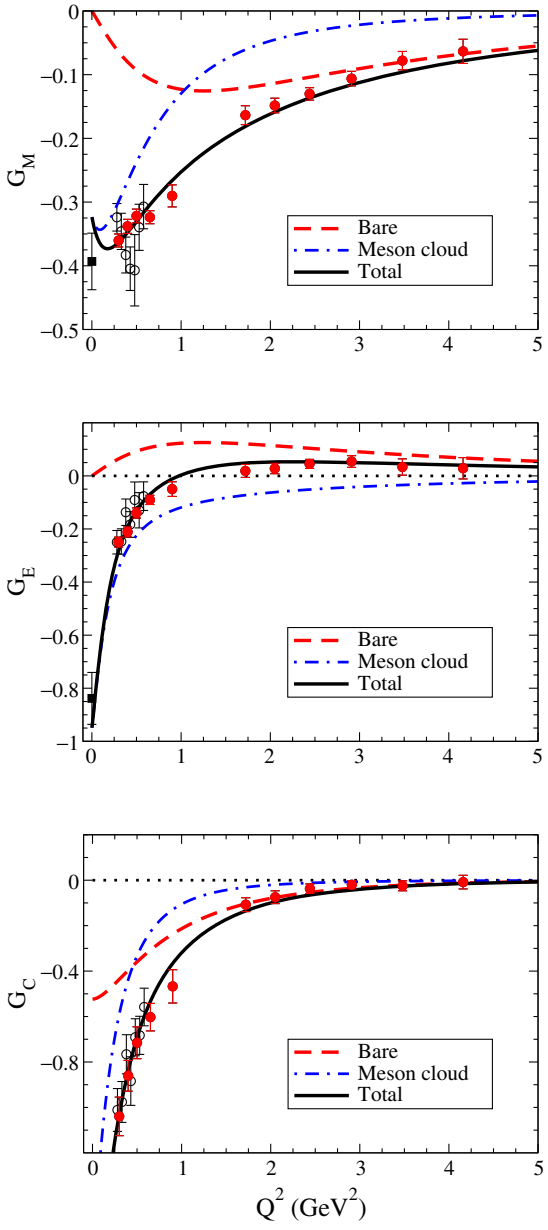

FIG. 3. Valence quark core plus meson cloud contributions to the spacelike form factors as a function of $Q^2 = -q^2$. Data come from Ref. [48] (the full circles), Ref. [49] (the empty circles), and PDG [50] (the square).

In our first work in Ref. [20] the meson cloud was different than the one that we are using here. The reason is that the meson model associated with Fig. 2(b) was, meanwhile, reparametrized in Ref. [7] to fix the incorrect position of the rho mass pole given by our first model, as well as by other popular parametrizations [7]. In addition, we notice that, in this new parametrization, the $\gamma^* N \to \Delta$ transition pion cloud is directly connected to the pion electromagnetic form factor $F_\pi(q^2)$, which is well established experimentally in the timelike region [7].

The parameters used in the formulas (5.22)–(5.24) were determined by their fit to the $\gamma^* N \to N^*(1520)$ spacelike form factors, giving $a_M = 5.531$ GeV^{-2}, $\lambda_\pi^{(4)} = -1.019$, $\lambda_\pi^M = -0.323$, $\lambda_\pi^C = -1.678$, $\Lambda_4^2 = 10.2$ GeV^2, $\Lambda_M^2 = 1.241$ GeV^2, and $\Lambda_C^2 = 1.263$ GeV^2. The results are presented in Fig. 3 as a function of $Q^2 = -q^2$ and compared with the spacelike data [48–50]. Check Ref. [20] for a more detailed discussion of the data. In the figure we also show the valence quark contributions (the dashed line) and the meson cloud contributions (the dashed-dotted line) based on the parametrizations described above.

In the Appendix, we discuss the technical aspects of the regularization of the singularities appearing in the multipoles of Eqs. (5.22)–(5.24).

VI. RESULTS

We present in this section our predictions for the $\gamma^* N \to N^*(1520)$ transition form factors in the timelike region. Using these results, we also calculate the γN and $e^+ e^- N$ decay widths.

A. Form factors

The predictions for the absolute values of the form factors G_M, G_E, and G_C in the timelike region are presented in Fig. 4 for the cases $W = 1.52$, 1.8, and 2.1 GeV. The valence quark core contributions are given by the thin lines. They stand very near the horizontal axis and vanish in the upper limit, $q^2 = (W - M)^2$, by kinematic constraints. The same result was observed in the quadrupole form factors of the $\gamma^* N \to \Delta(1232)$ transition for the physical case, when $W = M_\Delta \simeq 1.232$ GeV [51].

Figure 4 shows that the meson cloud contribution largely dominates. Only near the ω pole ($q^2 \simeq 0.6$ GeV^2) is there a significant contribution from the quark core for the absolute value of the form factors G_M and G_E. This effect is very concentrated near $q^2 \simeq m_\omega^2$ as a consequence of the small ω width, $\Gamma_\omega(m_\omega^2)$.

In G_C the effect of the ω pole is not observed. This is due to the cancellation of the isoscalar contributions to the form factor G_C. This cancellation is obtained analytically and can be confirmed by substituting the form factors G_1, G_2, G_3 given by Eqs. (5.14)–(5.16) into the formula of Eq. (5.10) for G_C. One concludes that only the quark isovector form factors, f_{1-} and f_{2-}, contribute to G_C.

From Fig. 4, one concludes that a fairly good description of the $\gamma^* N \to N^*(1520)$ transition can be obtained without the valence quark core contributions, which are very small. The almost perfect coincidence, both for G_M and G_E, of the lines corresponding to different values of W is also a consequence of the dominance of the meson cloud component since only the valence part depends on W. Only for G_C can one distinguish a slight W dependence, and this is evident because the valence quark contributions are nonzero when $q^2 = 0$. The main role of the mass dependence W in the behavior of the form factors is then to constrain them for $q^2 \leq (W - M)^2$.

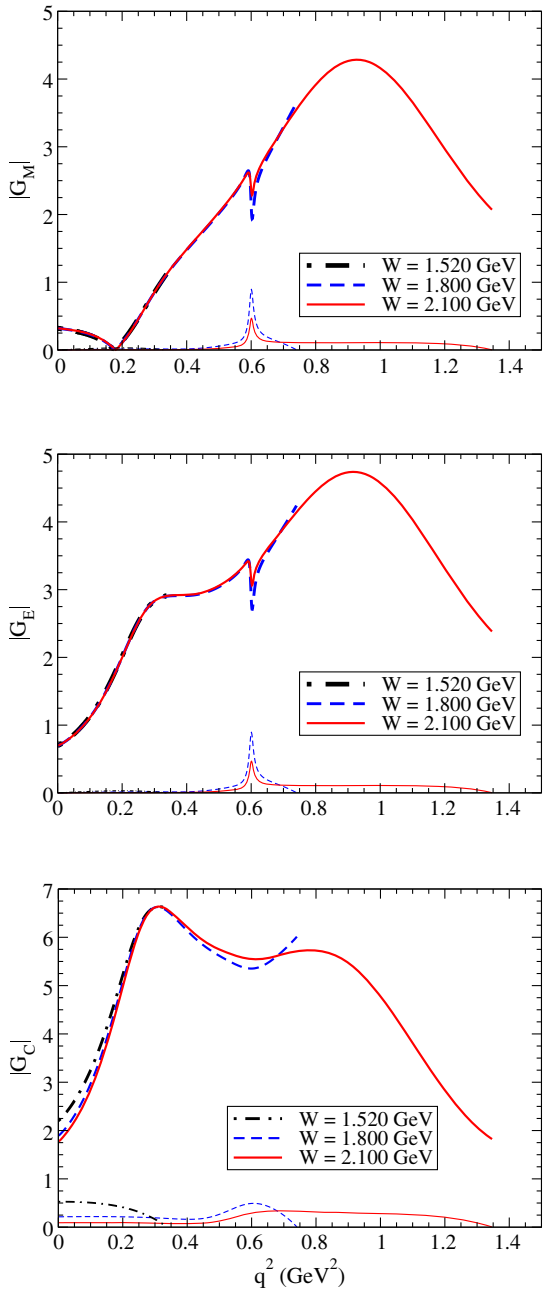

FIG. 4. Absolute values of the form factors for $W = 1.520$, 1.800, and 2.100 GeV. In the calculations we use the new parametrization and the width $\Gamma_\omega(q^2)$ given by Eq. (4.8). The thin lines represent the contribution from the core. For the total result (the thick lines), the lines for $W = 1.520$ GeV coincide with the lines for $W = 1.800$ and 2.100 GeV.

Qualitatively, one can say that the form factors are enhanced around the origin up to a certain maximum value of q^2. For $W = 2.1$ GeV, the magnitude of the form factors starts to decrease after $q^2 \approx 1$ GeV^2. This effect is a consequence of the meson cloud parametrization by Eqs. (5.22)–(5.24), which includes a cutoff for q^2 around 1.2 GeV^2. For larger values of W, the falloff of the form factors can also be observed.

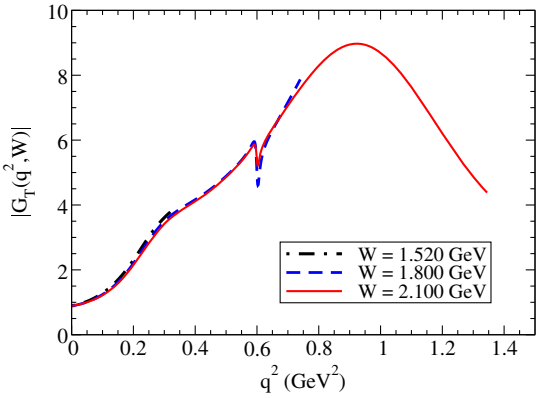

FIG. 5. Effective contribution of the form factors $|G_T(q^2, W)|$ for $W = 1.520$, 1.800, and 2.100 GeV.

The impact of the transition form factors in the timelike reactions is determined by the absolute value of $|G_T(q^2, W)|$ given by Eq. (3.3). The results for $|G_T(q^2, W)|$ for $W = 1.52$, 1.8, and 2.1 GeV are presented in Fig. 5. There is an increase of $|G_T(q^2, W)|$ relative to its value at the origin up to $q^2 \simeq 0.9$ GeV^2, for $W > 1.8$ GeV. Above $q^2 = 0.9$ GeV^2, one gets a first glance at the expected falloff for the form factors mentioned previously.

The function $|G_T(q^2, W)|$, particularly how it evolves away from $q^2 = 0$, has important consequences for the $N^*(1520) \to \gamma^* N$ transition. In general, the $N^* \to \gamma^* N$ reactions are often studied under the assumption that the transition form factors in the timelike region can be approximated by the experimental value of the form factors at the photon point ($q^2 = 0$), which implies that W is fixed by the physical mass of the resonance—and therefore there is no W dependence. In the literature, this approximation (no q^2 dependence of the electromagnetic coupling and $W = M_R$) is known as the QED approximation, and it represents the form factor of a pointlike particle. We also refer to this approximation as the constant form factor model. By construction, the constant form factor model is not constrained by the form factor G_C because, at $q^2 = 0$, G_C does not contribute to $|G_T|^2$, according to Eq. (3.3). For a finite q^2, however, G_C contributes to $|G_T|^2$ with the term $\frac{q^2}{2W^2}|G_C|^2$.

In Fig. 5, one can see that the value of $|G_T|$ at $q^2 = 0$ is close to 1, which is consistent with the experimental value. Therefore, in the constant form factor model, $|G_T| \equiv 1.048$ underestimates the results from Fig. 5. Taking, for instance, $q^2 = 0.9$ GeV, where $|G_T| \simeq 9$, one concludes that, in the constant form factor model, $|G_T|$ is about an order of magnitude too low. Since the impact of $|G_T|$ in the decay widths is proportional to $|G_T|^2$, in the range $q^2 = 0$–1 GeV^2, the constant form factor model may underestimate the decay widths in 1 or 2 orders of magnitude. For larger values of q^2, however, the discussion is different since, in our model, $|G_T|^2$ goes down with q^2

due to the multipole parametrizations of the meson cloud component.

The meson cloud dominance can be physically understood in terms of the decay mechanisms of the resonances $N^*(1520)$ and $\Delta(1232)$. The $\Delta(1232)$ decays almost exclusively into πN, but the $N^*(1520)$ can decay into πN (40%) and into $\pi\pi N$ (60%) [50]. From the $\pi\pi N$ decays, one can expect then a stronger contribution from the meson cloud effects for the transition form factors for the $N^*(1520)$ than for the $\Delta(1232)$. The strength of these $\pi\pi N$ decays is encoded in the form factor data that we use in our fit to the physical spacelike form factor data. In the $\gamma^* N \to \Delta(1232)$ transition, the leading form factor is the magnetic form factor, and in ours and other calculations, it is dominated by the valence quark contributions at low q^2's [6,7,22,23]. There is, therefore, a smaller impact from the pion cloud. By contrast, for the $\gamma^* N \to N^*(1520)$ transition, the electric and the magnetic form factors are both relevant at low q^2's. It is the different structure of form factors for the $\gamma^* N \to N^*(1520)$ and $\gamma^* N \to \Delta(1232)$ transition that implies a dominance of the meson cloud effects, in the first case.

B. Calculation of the decay width $\Gamma_{\gamma N}(W)$

Using the formalism in Sec. III, we calculate the $N^*(1520) \to \gamma N$ decay width as a function of W. The γN decay width ($\Gamma_{\gamma N}$) is determined by the function $\Gamma_{\gamma^* N}(q, W)$, given by Eq. (3.1) in the limit $q^2 = 0$. This width is then proportional to the function $|G_T(0, W)|^2$.

Our results for $\Gamma_{\gamma N}(W)$ are presented in Fig. 6 (the thick solid line). Since, as observed for the form factors, the dependence of $|G_T|$ on W is weak, the shape of $\Gamma_{\gamma N}(W)$ is determined mainly by the kinematic factor multiplying $|G_T|^2$ in Eq. (3.1). The results are also compared with the constant form factor model (the dashed line). In the figure, the results from the constant form factor for $\Gamma_{\gamma N}(W)$ are close to the q^2 dependent results, but we note that a logarithmic representation is used. The deviation for large W's is about 30%. The similarity between the two results comes from the small dependence of our model on W in the limit $q^2 \to 0$. We expect that, for observables depending on q^2, the results will differ much more. This is indeed the case, as confirmed in the next section.

To close this section, we compare $\Gamma_{\gamma N}(W)$ with the $\Delta(1232) \to \gamma N$ decay width calculated in Ref. [7], which is also within the covariant spectator quark model framework (the thin solid line). It is interesting that the Δ decay width is larger for small values of W, but the $N^*(1520)$ decay width is larger when $W > 2.5$ GeV.

C. $N^*(1520)$ Dalitz decay

We show now the results for the $N^*(1520)$ Dalitz decay, $N^*(1520) \to e^+e^-N$. The Dalitz decay width is determined by the function $\Gamma_{\gamma^* N}(q, W)$, given by Eq. (3.1) for the case

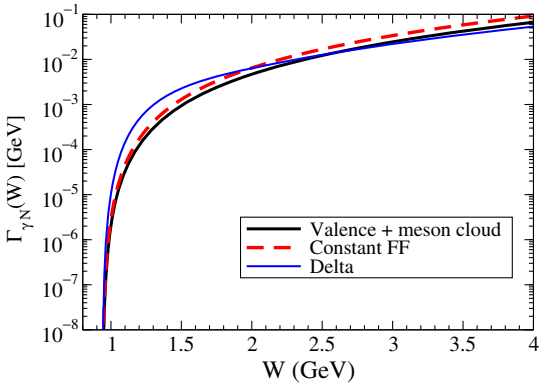

FIG. 6. Decay width $\Gamma_{\gamma N}$ as function of W. The current model (Valence + meson cloud) is compared with the constant form factor model and with the results obtained for the $\Delta(1232)$ (see Ref. [7]).

where q^2 is the photon momentum transfer for the dilepton decay $\gamma^* \to e^+e^-$.

In Fig. 7, we present the results of $\Gamma_{\gamma^* N}(q, W)$ for $W = 1.52$, 1.8, and 2.1 GeV. The dependence of $\Gamma_{\gamma^* N}$ on both variables, q^2 and W, is clear from the figure.

Finally, we show the dilepton decay rate $\frac{d\Gamma}{dq}(q, W)$, where, as before, we use the notation $\Gamma(q, W) \equiv \Gamma_{e^+e^-N}(q, W)$. The results for $\frac{d\Gamma}{dq}$ for the three values of W discussed previously are presented in Fig. 8. The results are compared with the constant form factor model. The covariant spectator quark model differs significantly from the constant form factor model for $q^2 > 0.1$ GeV^2. This effect is caused by the meson cloud contributions included in our model.

The function $\Gamma_{e^+e^-N}(W)$ can now be evaluated by integrating q according to Eq. (3.5). The results are presented in Fig. 9, which also shows a comparison to the results obtained with the constant form factor model. From the figure, we can conclude that the effect of the q^2 dependence is diluted when we integrate q for $W < 1.6$ GeV. One concludes then that the q^2 dependence

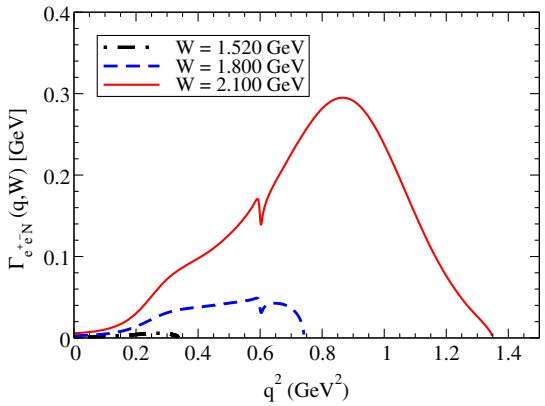

FIG. 7. Dalitz decay width $\Gamma_{e^+e^-N}(q^2, W)$ for $W = 1.520$, 1.800, and 2.100 GeV.

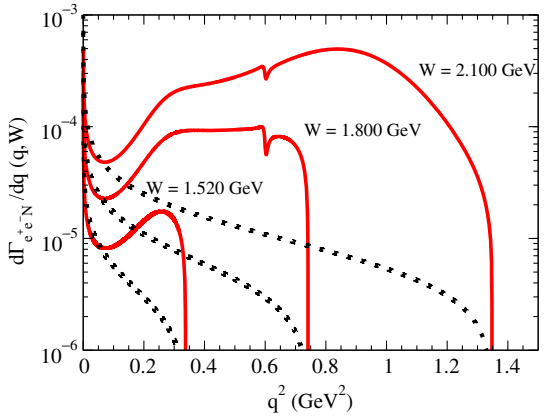

FIG. 8. Results of $\frac{d\Gamma}{dq}$ for $W = 1.520$, 1.800, and 2.100 GeV (the solid lines) compared to the estimate from the constant form factor model (the dotted lines).

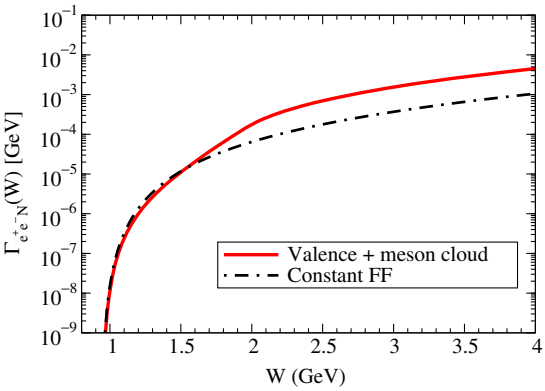

FIG. 9. $N^*(1520)$ Dalitz decay width as a function of W. The result of our model (the solid line) is compared to the result of the constant form factor model (the dotted-dashed line).

on $|G_T|^2$ is important when we look for the function $\Gamma_{e^+e^-N}(q,W)$, or for $\Gamma_{e^+e^-N}(W)$ at a large W.

In Fig. 10 we present the results of $\Gamma_{e^+e^-N}(W)$ in comparison to the electromagnetic decay width $\Gamma_{\gamma N}(W)$.

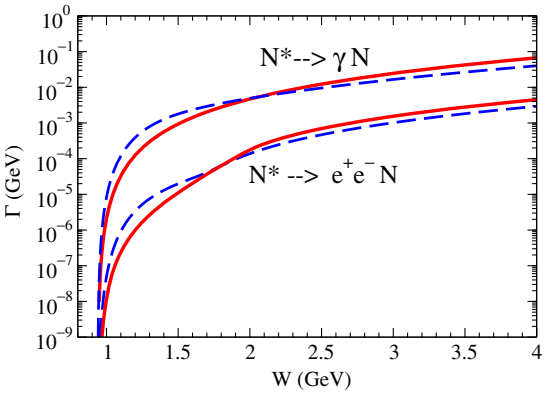

FIG. 10. $N^*(1520)$ decay widths as a function of W. Photon and Dalitz decays (the solid lines). The results are also compared to the calculation for the $\Delta(1232)$ case (the dashed lines).

In the same figure, we also compare our results for $\Gamma_{e^+e^-N}(W)$, $\Gamma_{\gamma N}(W)$ from the $N^*(1520)$ resonance to the corresponding ones from the $\Delta(1232)$ decays [7]. In both cases, one includes the combination of the valence quark and meson cloud contributions.

The results from Fig. 10 imply that the two resonances are almost equally relevant for a large W, suggesting that the $N^*(1520)$ may play an important role in dilepton decay reactions.

VII. OUTLOOK AND CONCLUSIONS

We apply to the $N^*(1520) \to \gamma N$ transition a model which adds a covariant valence quark core contribution with a meson cloud term. The meson cloud term is related to the pion electromagnetic form factor, which is well established in the timelike region, and the transition form factors are first fixed in the spacelike region. The form factor behavior in the timelike region is then predicted, as is the $N^*(1520) \to \gamma N$ decay width and the $N^*(1520)$ Dalitz decay, $N^*(1520) \to e^+e^-N$. The timelike $N^*(1520)$ transition form factors are dominated by the meson cloud contributions.

In the range $q^2 = 0$–1 GeV^2, the constant form factor model, or QED approximation, that is usually taken in the literature underestimates the electromagnetic coupling of the $N^*(1520)$ up to 2 orders of magnitude. This has a large effect on q^2 dependent observables as the $N^*(1520)$ Dalitz decay. The q^2 dependence effect may be diluted in $\Gamma_{e^+e^-N}(W)$, which is obtained by integrating over q^2, but it can be clearly observed if we look at the differential Dalitz decay width $\frac{d\Gamma}{dq}(q,W)$.

In line with the HADES results [3,13,14], the $N^*(1520)$ and $\Delta(1232)$ decays compete, and at large energies the former is certainly important.

ACKNOWLEDGMENTS

G. R. was supported by the Brazilian Ministry of Science, Technology and Innovation (MCTI-Brazil). M. T. P. received financial support from Fundação para a Ciência e a Tecnologia (FCT) under Grants No. PTDC/FIS/113940/2009, No. CFTP-FCT (PEst-OE/FIS/U/0777/2013), and No. POCTI/ISFL/2/275. This work was also partially supported by the European Union under HadronPhysics3 Grant No. 283286.

APPENDIX: REGULARIZATION OF HIGH MOMENTUM POLES

As discussed in the main text, for a given W, the squared momentum q^2 is limited by the condition $q^2 \leq (W-M)^2$. Then, if one has a singularity for $q^2 = \Lambda^2$, that singularity will appear for values of W, such that $\Lambda^2 \leq (W-M)^2$, or $W \geq M + \Lambda$.

To avoid a singularity at $q^2 = \Lambda^2$, where Λ^2 is one of the cutoffs introduced in our meson cloud parametrizations and in the quark current (the pole at $q^2 = M_h$) we will use a simple procedure. We start with

$$\frac{\Lambda^2}{\Lambda^2 - q^2} \to \frac{\Lambda^2}{\Lambda^2 - q^2 - i\Lambda\Gamma_X(q^2)}, \tag{A1}$$

where

$$\Gamma_X(q^2) = 4\Gamma_X^0 \left(\frac{q^2}{q^2 + \Lambda^2}\right)^2 \theta(q^2). \tag{A2}$$

In the last equation, Γ_X^0 is a constant given by $\Gamma_X^0 = 4\Gamma_\rho^0 \simeq 0.6$ GeV.

The function $\Gamma_X(q^2)$ defined by Eq. (A2) is $\Gamma_X(q^2) = 0$ when $q^2 < 0$ and is continuously extended for $q^2 > 0$. Therefore, the results in the spacelike region (where there are no singularities) are kept unchanged. The factor $4\Gamma_X^0$ was chosen in order to obtain $\Gamma_X = \Gamma_X^0$ for $q^2 = \Lambda^2$, and $\Gamma_X \simeq 4\Gamma_X^0$ for very large q^2's. Finally the value of Γ_X^0 was chosen to avoid very narrow peaks around Λ^2.

Unlike the width $\Gamma_\rho(q^2)$ associated with the ρ-meson pole in the quark current, which has nonzero values only when $q^2 > 4m_\pi^2$, one also has nonzero values for $\Gamma_X(q^2)$ in the interval $4m_\pi^2 > q^2 > 0$. However, the function $\Gamma_X(q^2)$ varies smoothly in that interval, and its values are very small when compared to Γ_X^0.

The procedure given by Eqs. (A1) and (A2) was used already in applications of the model from Ref. [6] in the calculation of the $\gamma^* N \to \Delta$ form factors in the timelike regime [7,17]. With this procedure, the emerging singularities for $W > 2.17$ GeV are avoided and the results are almost identical to the results for $W < 2.17$ GeV, without regularization. The singularity that appears for $W \simeq 2.17$ GeV is due to the pion cloud parametrization of G_M [6].

As in most cases, the high momentum effects and the high q^2 contributions are suppressed, and the details of the regularization procedure are not important as far as removing the spurious singularities is concerned.

For the tripole factors associated with the functions (5.22)–(5.24), we use

$$\left(\frac{\Lambda^2}{\Lambda^2 - q^2}\right)^3 \to \left(\frac{\Lambda^4}{(\Lambda^2 - q^2)^2 + \Lambda^2[\Gamma_X(q^2)]^2}\right)^{3/2}, \tag{A3}$$

where $\Gamma_X(q^2)$ is obtained by Eq. (A2).

[1] W. J. Briscoe, M. Döring, H. Haberzettl, D. M. Manley, M. Naruki, I. I. Strakovsky, and E. S. Swanson, Physics opportunities with meson beams, Eur. Phys. J. A **51**, 129 (2015).

[2] A. Faessler, C. Fuchs, M. I. Krivoruchenko, and B. V. Martemyanov, Dilepton production in proton proton collisions at BEVALAC energies, J. Phys. G **29**, 603 (2003).

[3] G. Agakishiev *et al.*, Baryon resonance production and dielectron decays in proton-proton collisions at 3.5 GeV, Eur. Phys. J. A **50**, 82 (2014); Inclusive dielectron spectra in $p + p$ collisions at 3.5 GeV, Eur. Phys. J. **48**, 64 (2012).

[4] G. Agakishiev *et al.* (HADES Collaboration), Study of exclusive one-pion and one-eta production using hadron and dielectron channels in pp reactions at kinetic beam energies of 1.25 GeV and 2.2 GeV with HADES, Eur. Phys. J. A **48**, 74 (2012); Inclusive dielectron production in proton-proton collisions at 2.2 GeV beam energy, Phys. Rev. C **85**, 054005 (2012); Analysis of pion production data measured by HADES in proton-proton collisions at 1.25 GeV, Eur. Phys. J. A **51**, 137 (2015).

[5] G. Agakishiev *et al.* (HADES Collaboration), Origin of the low-mass electron pair excess in light nucleus-nucleus collisions, Phys. Lett. B **690**, 118 (2010); First measurement of proton-induced low-momentum dielectron radiation off cold nuclear matter, Phys. Lett. B **715**, 304 (2012).

[6] G. Ramalho and M. T. Peña, Timelike $\gamma^* N \to \Delta$ form factors and Δ Dalitz decay, Phys. Rev. D **85**, 113014 (2012).

[7] G. Ramalho, M. T. Peña, J. Weil, H. van Hees, and U. Mosel, Role of the pion electromagnetic form factor in the $\Delta(1232) \to \gamma^* N$ timelike transition, Phys. Rev. D **93**, 033004 (2016).

[8] I. G. Aznauryan, A. Bashir, V. Braun, S. J. Brodsky, V. D. Burkert, L. Chang, C. Chen, B. El-Bennich *et al.*, Studies of nucleon resonance structure in exclusive meson electroproduction, Int. J. Mod. Phys. E **22**, 1330015 (2013).

[9] I. G. Aznauryan and V. D. Burkert, Electroexcitation of nucleon resonances, Prog. Part. Nucl. Phys. **67**, 1 (2012).

[10] S. Teis, W. Cassing, M. Effenberger, A. Hombach, U. Mosel, and G. Wolf, Pion production in heavy ion collisions at SIS energies, Z. Phys. A **356**, 421 (1997).

[11] S. A. Bass *et al.*, Microscopic models for ultrarelativistic heavy ion collisions, Prog. Part. Nucl. Phys. **41**, 255 (1998).

[12] O. Buss, T. Gaitanos, K. Gallmeister, H. van Hees, M. Kaskulov, O. Lalakulich, A. B. Larionov, T. Leitner, J. Weil, and U. Mosel, Transport-theoretical description of nuclear reactions, Phys. Rep. **512**, 1 (2012).

[13] B. Ramstein (for the HADES Collaboration), Studying time-like baryonic transitions with HADES, AIP Conf. Proc. **1735**, 080001 (2016).
[14] W. Przygoda (for the HADES Collaboration), Resonance production and decay in proton and pion induced collisions with HADES, J. Phys. Soc. Jpn. Conf. Proc. **10**, 010013 (2016).
[15] E. L. Bratkovskaya, W. Cassing, M. Effenberger, and U. Mosel, e^+e^- production from pp reactions at BEVALAC energies, Nucl. Phys. **A653**, 301 (1999).
[16] L. P. Kaptari and B. Kampfer, Di-electrons from resonances in nucleon-nucleon collisions, Phys. Rev. C **80**, 064003 (2009).
[17] J. Weil, H. van Hees, and U. Mosel, Dilepton production in proton-induced reactions at SIS energies with the GiBUU transport model, Eur. Phys. J. A **48**, 111 (2012); **48**, 150(E) (2012).
[18] G. Eichmann, H. Sanchis-Alepuz, R. Williams, R. Alkofer, and C. S. Fischer, Baryons as relativistic three-quark bound states, Prog. Part. Nucl. Phys. **91**, 1 (2016).
[19] F. Gross, Three-dimensional covariant integral equations for low-energy systems, Phys. Rev. **186**, 1448 (1969); A. Stadler, F. Gross, and M. Frank, Covariant equations for the three-body bound state, Phys. Rev. C **56**, 2396 (1997).
[20] G. Ramalho and M. T. Peña, $\gamma^*N \to N^*(1520)$ form factors in the spacelike region, Phys. Rev. D **89**, 094016 (2014).
[21] F. Gross, G. Ramalho, and M. T. Peña, Pure S-wave covariant model for the nucleon, Phys. Rev. C **77**, 015202 (2008).
[22] G. Ramalho, M. T. Peña, and F. Gross, A covariant model for the nucleon and the Δ, Eur. Phys. J. A **36**, 329 (2008).
[23] G. Ramalho, M. T. Peña, and F. Gross, D-state effects in the electromagnetic $N\Delta$ transition, Phys. Rev. D **78**, 114017 (2008).
[24] F. Gross, G. Ramalho, and M. T. Peña, Spin and angular momentum in the nucleon, Phys. Rev. D **85**, 093006 (2012).
[25] F. Gross, G. Ramalho, and M. T. Peña, Covariant nucleon wave function with S-, D-, and P-state components, Phys. Rev. D **85**, 093005 (2012).
[26] G. Ramalho, K. Tsushima, and F. Gross, Relativistic quark model for the Ω^- electromagnetic form factors, Phys. Rev. D **80**, 033004 (2009).
[27] G. Ramalho and M. T. Peña, Extracting the Ω^- electric quadrupole moment from lattice QCD data, Phys. Rev. D **83**, 054011 (2011).
[28] G. Ramalho, M. T. Peña, and A. Stadler, Shape of the Δ baryon in a covariant spectator quark model, Phys. Rev. D **86**, 093022 (2012); G. Ramalho, M. T. Peña, and F. Gross, Electromagnetic form factors of the Δ with D-waves, Phys. Rev. D **81**, 113011 (2010); G. Ramalho and M. T. Peña, Electromagnetic form factors of the Δ in an S-wave approach, J. Phys. G **36**, 085004 (2009).
[29] G. Ramalho and K. Tsushima, $\gamma^*N \to N(1710)$ transition at high momentum transfer, Phys. Rev. D **89**, 073010 (2014); Valence quark contributions for the $\gamma N \to P_{11}(1440)$ form factors, Phys. Rev. D **81**, 074020 (2010)
[30] G. Ramalho and M. T. Peña, Covariant model for the $\gamma N \to N(1535)$ transition at high momentum transfer, Phys. Rev. D **84**, 033007 (2011).
[31] G. Ramalho and K. Tsushima, Model for the $\Delta(1600)$ resonance and $\gamma N \to \Delta(1600)$ transition, Phys. Rev. D **82**, 073007 (2010).
[32] G. Ramalho, Using the single quark transition model to predict nucleon resonance amplitudes, Phys. Rev. D **90**, 033010 (2014).
[33] G. Ramalho and K. Tsushima, Axial form factors of the octet baryons in a covariant quark model, Phys. Rev. D **94**, 014001 (2016).
[34] G. Ramalho and M. T. Peña, Nucleon and $\gamma N \to \Delta$ lattice form factors in a constituent quark model, J. Phys. G **36**, 115011 (2009).
[35] G. Ramalho and M. T. Peña, Valence quark contribution for the $\gamma N \to \Delta$ quadrupole transition extracted from lattice QCD, Phys. Rev. D **80**, 013008 (2009).
[36] F. Gross, G. Ramalho, and K. Tsushima, Using baryon octet magnetic moments and masses to fix the pion cloud contribution, Phys. Lett. B **690**, 183 (2010); G. Ramalho and K. Tsushima, Octet baryon electromagnetic form factors in a relativistic quark model, Phys. Rev. D **84**, 054014 (2011).
[37] G. Ramalho, D. Jido, and K. Tsushima, Valence quark and meson cloud contributions for the $\gamma^*\Lambda \to \Lambda^*$ and $\gamma^*\Sigma^0 \to \Lambda^*$ reactions, Phys. Rev. D **85**, 093014 (2012); G. Ramalho and K. Tsushima, Covariant spectator quark model description of the $\gamma^*\Lambda \to \Sigma^0$ transition, Phys. Rev. D **86**, 114030 (2012); What is the role of the meson cloud in the $\Sigma^{*0} \to \gamma\Lambda$ and $\Sigma^* \to \gamma\Sigma$ decays?, Phys. Rev. D **88**, 053002 (2013); Octet to decuplet electromagnetic transition in a relativistic quark model, Phys. Rev. D **87**, 093011 (2013).
[38] G. Ramalho, K. Tsushima, and A. W. Thomas, Octet baryon electromagnetic form factors in nuclear medium, J. Phys. G **40**, 015102 (2013).
[39] M. I. Krivoruchenko, B. V. Martemyanov, A. Faessler, and C. Fuchs, Electromagnetic transition form factors and dilepton decay rates of nucleon resonances, Ann. Phys. (Amsterdam) **296**, 299 (2002).
[40] A. Faessler, C. Fuchs, and M. I. Krivoruchenko, Dilepton spectra from decays of light unflavored mesons, Phys. Rev. C **61**, 035206 (2000).
[41] J. J. Kelly, Gauge ambiguities in $(\vec{e} \to e'\vec{N})$ reactions, Phys. Rev. C **56**, 2672 (1997).
[42] Z. Batiz and F. Gross, Pole term and gauge invariance in deep inelastic scattering, Phys. Rev. C **58**, 2963 (1998).
[43] R. A. Gilman and F. Gross, Electromagnetic structure of the deuteron, J. Phys. G **28**, R37 (2002).
[44] P. Mühlich and U. Mosel, ω attenuation in nuclei, Nucl. Phys. **A773**, 156 (2006); P. Mühlich, Ph.D. thesis, University of Giessen, 2007.
[45] H. B. O'Connell, B. C. Pearce, A. W. Thomas, and A. G. Williams, ρ-ω mixing and the pion electromagnetic form-factor, Phys. Lett. B **354**, 14 (1995).
[46] H. B. O'Connell, B. C. Pearce, A. W. Thomas, and A. G. Williams, ρ-ω mixing, vector meson dominance and the pion form-factor, Prog. Part. Nucl. Phys. **39**, 201 (1997).
[47] R. C. E. Devenish, T. S. Eisenschitz, and J. G. Korner, Electromagnetic $N - N^*$ transition form factors, Phys. Rev. D **14**, 3063 (1976).

[48] I. G. Aznauryan *et al.* (CLAS Collaboration), Electroexcitation of nucleon resonances from CLAS data on single pion electroproduction, Phys. Rev. C **80**, 055203 (2009).

[49] V. I. Mokeev *et al.* (CLAS Collaboration), Experimental study of the $P_{11}(1440)$ and $D_{13}(1520)$ resonances from CLAS data on $ep \to e'\pi^+\pi^- p'$, Phys. Rev. C **86**, 035203 (2012).

[50] J. Beringer *et al.* (Particle Data Group Collaboration), Review of Particle Physics, Phys. Rev. D **86**, 010001 (2012).

[51] G. Ramalho, Parametrizations of the $\gamma^* N \to \Delta(1232)$ quadrupole form factors and Siegert's theorem, Phys. Rev. D **94**, 114001 (2016).